RESEARCH ARTICLE

External electric field effect on hydrogen adsorption and storage on a Palladium-functionalized C_{20} bowl: A computational investigation

Sonia Shayanmehr[1], Reza Ghiasi[2,*], Behrooz Mirza[1], Bita Mohtat[1]

[1]*Department of Chemistry, Karaj Branch, Islamic Azad University, Karaj, Iran*

[2]*Department of Chemistry, East Tehran Branch, Islamic Azad University, Tehran, Iran*

ARTICLE INFO

Article History:
Received 2022-09-26
Accepted 2024-06-12
Published 2023-05-05

Keywords:
C_{20} bowl,
Hydrogen storage,
Adsorption,
External Electric Field (EEF).

ABSTRACT

This study investigated the adsorption of hydrogen molecule on a palladium-functionalized C_{20} bowl in the absence and presence of an external electric field (EEF) along the z-axis using the B3LYP-D3 model. The EEF effect on the stability of the different isomers of hydrogen adsorption was investigated. In the absence and presence of EEF, the **I**-isomer was a more stable isomer compared to the **II**-isomer. In these systems, the corrected adsorption energy amounts are estimated. Alterations in the dipole moment as well as structural factors were displayed in the presence and absence of EEF. The effects of EEF strength on electronic and structural factors were studied. Also, the H-H stretching wavenumber (ν_{H-H}) of the studied systems was calculated. Larger ν_{H-H} values were found in the presence of EEF than in the absence of EEF. Linear correlations between adsorption energy, relative energy, dipole moment, and ν_{H-H} values with EEF strength were provided.

How to cite this article

Shayanmehr S., Ghiasi R., Mirza B., Mohtat B., External electric field effect on hydrogen adsorption and storage on a Palladium-functionalized C20 bowl: A computational investigation. J. Nanoanalysis., 10 (2): 505-514, Spring 2023.

INTRODUCTION

Hydrogen is the most common and simple chemical element, consisting of only one electron and one proton. Hydrogen is produced by renewable raw materials, particularly natural gas, as the most cost-effective candidate for hydrogen supply [1]. It demonstrates high sustainability, renewability, and energy efficiency. It is a clean energy carrier, and hydrogen combustion in the fuel cell generates power, heat or electricity with no pollution of the environment or effect on the climate [2]. So, hydrogen can be considered an energy carrier for transportation systems

*Corresponding Author Email: *reza.ghiasi@iau.ac.ir*

like aircraft and vehicles.

In normal circumstances, hydrogen is a highly volatile gas that should be stored in fuel-cells for practical uses. It can be stored as either a liquid (cryogenic temperature) or a gas (by high-pressure, 5000–10000 psi tank pressure) on board a vehicle [3]. Therefore, adequate transportation and storage techniques are essential to applying hydrogen as a fuel in fuel-cell systems. Its safety and storage challenges on fuel cell vehicles (as a lightweight, small, and immune container) are important problems for hydrogen fuel cars [4, 5]. Various computational investigations have been reported about hydrogen storage in different systems [6-14]. In a computational investigation, hydrogen storage and adsorption on Palladium-functionalized graphene as well as hydrogen the boron nitride analogue were investigated [15]. A density functional theory investigation on $(Mg(BH_4))n$ (n = 1–4) clusters to be used as a material for hydrogen storage has been published [16].

Fullerene is an allotrope of carbon and is composed of individual molecules characterized by an infinite number of discrete. Fullerene was detected after graphite and diamond, and in contrast to graphite and diamond, each Fullerene type possesses its own specific features [17]. Fullerene is commonly generated by pyrolysis, electric arc vaporization, combustion, or laser ablation [18-22]. Cage, bowl, and ring are the lowest energy members in the C_{20} family. Although fullerene is not soluble in water, it shows limited solubility in conventional organic solvents [23]. It partially masks the polar fullerene surface or covalently modifies the aromatic structure to overcome its compatibility restriction with biological media [23]. A computational investigation of hydrogen adsorption and storage on palladium-functionalized C_{20} bowl and $C_{20}H_{10}$ bowl molecules including hydrogen saturation, has been reported [24].

The external electric fields (EEFs) impact the variations matching the geometric and electronic structure of many conjugated molecules; the chemical reactivity as well as the global and local reactivity measures were displayed [25-39].

In this work, we study the adsorption of hydrogen molecule on a palladium-functionalized C_{20} bowl in the presence and absence of EEF along the z-axis using the B3LYP-D3 model. The EEF effect on the structural and electronic parameters of the complex has been assessed.

COMPUTIONAL TECHNIQUES

We used Gaussian 09 software for data analysis [40]. The Def2-TZVPPD basis set [41-46] and the standard 6-311G(d,p) basis set [42-44, 47-51] were employed respectively for the Pt element and main groups of elements. The evaluated molecules were regarded in the singlet and neutral forms. For excluding direct computation of the correlation and exchange integrals of 18 electrons for the Pd atom, effective core potential (ECP) to the Def2-TZVPPD basis set employed [52].

B3LYP-D3 model was used for Geometry optimizations. B3LYP-D3 model can maintain the B3LYP method benefit and also it can simulate the weak interactions well using Grimme term D3 [53].

For proving no imaginary frequency of the optimized structures, harmonic vibrational frequencies computed.

RESULTS AND DISCUSSION

Energetic aspect

Figure 1 indicates structures of C_{20} bowl and two mode adsorption of hydrogen molecule on the Pd-doped C_{20} bowl. Optimized geometries of various modes of adsorption of hydrogen molecule on the Pd doped-C_{20}-bowl are displayed in Figure 2. The absolute energy as well as relative energy values of these isomers are computed in the absence and presence of

EEF along z-axis (Table 1). Such values indicate **I**-isomer is most energetically stable isomer both in presence and absence of EEF. Relative energy values are decreased with increasing of EEF strength. There are good linear correlations relative energy values with EEF strength (Figure 3).

$\Delta E = -288.32\ E_z + 34.06$;

$R^2 = 0.9861$

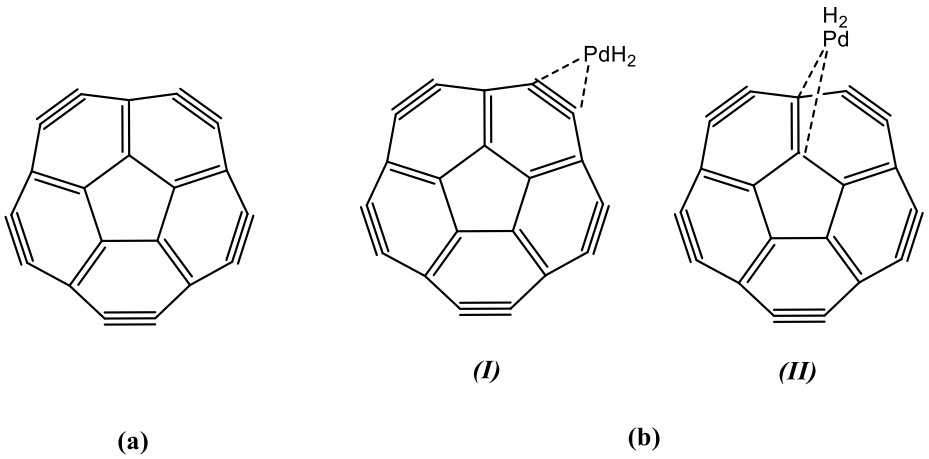

Figure 1. Structures of (a) C_{20} bowl (b) two mode adsorption of hydrogen molecule on the Pd-doped C_{20} bowl

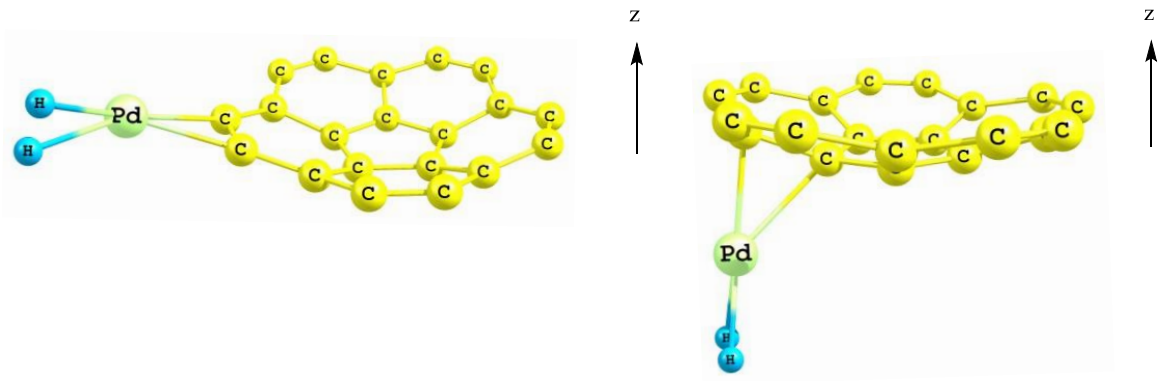

Figure 2. Optimized geometrized of the various isomers of $C_{20}PdH_2$ complex.

1. Adsorption energy values

The adsorption energy (ΔE_{ad}) can be assessed as follows:

$$\Delta E_{ad} = E(Pd - doped\ C_{20} \ldots H_2) - E(Pd - doped\ C_{20}) - E(H_2)$$

E (Pd-doped C_{20}-bowl) indicates the energy related to the isolated Pd-doped C_{20}-bowl; E (H_2) represents the hydrogen molecule energy, and E (Pd-doped C_{20}-bowl…H_2) indicates the energy related to hydrogen adsorbed on the Pd-doped C_{20}-bowl surface.

Corrected adsorption energy is calculated as follows:

$$\Delta E_{ad}^{corr} = \Delta E_{ad} + E(BSSE)$$

Where E indicates the basis set superposition error (BSSE) corrected for adsorption energy [54, 55].

The Corrected adsorption energy values of many isomers of adsorption of hydrogen molecule on the Pd-doped C_{20}-bowl are computed in the absence and presence of the EEF along the z-axis (Table 1). The negative ΔE_{ad} values indicate the desirable complex generation energetically. The range of calculated ΔE_{ad} values is acceptable for chemisorption. The adsorption energies indicate that the tendency to adsorb hydrogen molecule decreases with an increase in EEF strength along the z-axis Adsorption of hydrogen on the Pd-doped C_{20} bowl is stronger in the I-isomer than the II-isomer in the absence of EEF along the z-axis. Identical is observed in the presence of EEF at 0.001-0.007 a.u. But, stronger hydrogen adsorption occurs in the II-isomer than the I-isomer in the presence of EEF at 0.009-0.011 a.u. There are good linear correlations between corrected adsorption energy values and EEF strength (Figure 4).

ΔE_{ad}^{corr} $(I-isomer)$ = 26.756 E_z - 15.766;

R^2 = 0.9961

ΔE_{ad}^{corr} $(II-isomer)$ = 146.01 E_z - 16.717;

R^2 = 0.9716

2. Dipole moment

Dipole moment values related to evaluated molecules are measured in the presence and absence of EEF along the z-axis (Table 1). The more stable isomer (**I**-isomer) of adsorption of hydrogen molecule on the Pd-doped C_{20} bowl possesses the larger dipole moment value in absence and the presence of EEF at 0.001-0.007 a.u. II-isomer indicates larger dipole moment values in the presence of EEF at 0.009-0.011 a.u than I-isomer. Linear correlations between dipole moment values and EEF strength are:

μ (I-isomer) = 84.47 E_z + 4.0282;

R^2 = 0.8936

μ(II-isomer) = 356.83 E_z + 1.5751;

R^2 = 0.9973

It can be found, better linear relationship between two parameters for the II-isomer in compared to the I-isomer.

3. Structural parameters

Pd-C, H…H, and Pd-H distances in the Pd-doped C_{20} bowl complexes are summarized in Table 1 after and before hydrogen adsorption. It can be observed that the average of Pd-C bond distances and H-H bond lengths is shorter in the EEF presence alone z-axis than in the absence of EEF. These bond distances decrease with an increase in EEF strength. In the case of hydrogen adsorption, longer H-H distances are found compared to free hydrogen (74.4 pm).

Also, the mean Pd-H bond distances are longer in the EEF presence alone z-axis in comparison with the absence of EEF. Such bond distances are increased with an increase of EEF strength. Vibrational analysis

Vibrational analysis of the $C_{20}PdH_2$ complexes is investigated in the presence and absence of EEF along the a-axis. It can be found that the largest wavenumber is attributed to H-H stretching (ν_{H-H}). The wavenumber values of this vibration are listed in Table 2. Free hydrogen molecule reveals H-H stretching at 4419.4 cm^{-1} at B3LYP-D3/6-311G (d,P) level of theory. It can be observed that the position of this vibration is shifted to lower energy values after hydrogen adsorption occurs. Larger ν_{H-H} values are observed in the presence of EEF in comparison the absence of EEF. Such values enhance with an increase in EEF strength along the z-axis. The ν_{H-H} values are associated with EEF strength along z-axis (Figure 5).

ν_{H-H} (I-isomer) = 5723.5 E_z + 3479.6;

R^2 = 0.9976

ν_{H-H} (II-isomer) = 19987 E_z + 3425.4;

R^2 = 0.9963

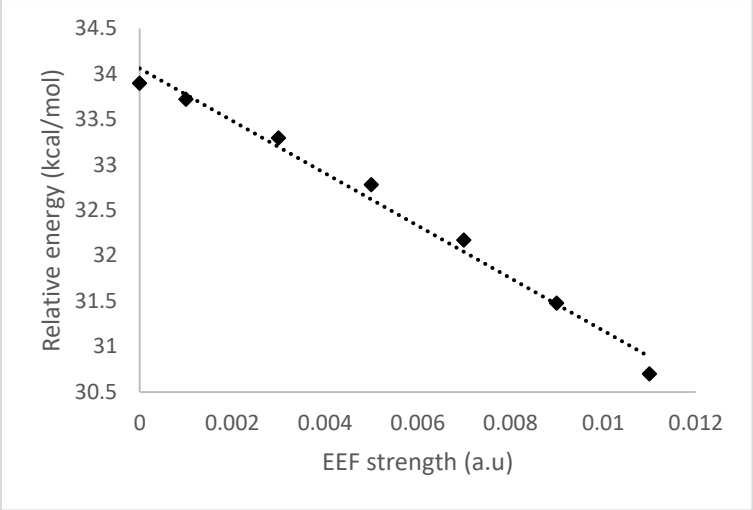

Figure 3. Linear correlations relative energy values of in the various $C_{20}PdH_2$ complexes with EEF strength along z-axis.

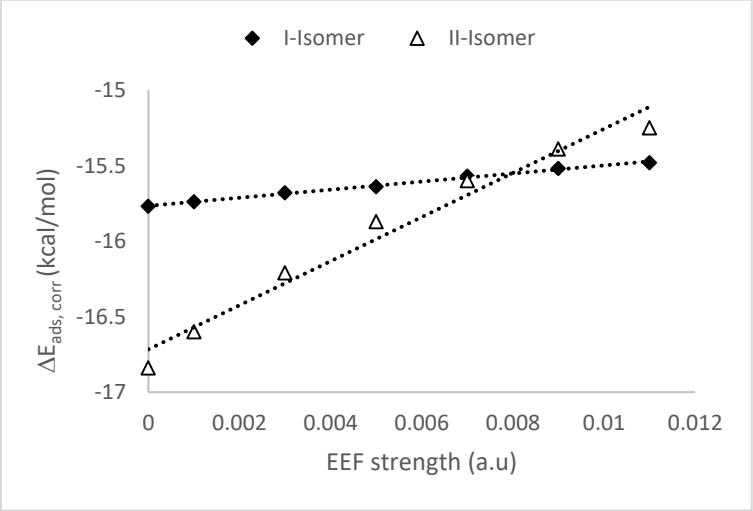

Figure 4. Linear correlations between corrected adsorption energy values with EEF strength along z-axis in the various $C_{20}PdH_2$ complexes.

Table 1. Energy (E, a.u), relative energy (ΔE, kcal/mol), corrected adsorption energy and dipole moment (μ, Debye) values of the two modes of adsorption hydrogen molecule on the Pd-doped C_{20} bowl in absence and presence of external electric filed along z-axis with E_z strength (in a.u).

E_z	E(I)	E(II)	ΔE(I)	ΔE(II)	$\Delta E_{ad}^{corr}(I)$	$\Delta E_{ad}^{corr}(II)$	μ(I)	μ(II)
0	-890.8959	-890.8419	0.00	33.90	-15.77	-16.84	4.1652	1.6835
0.001	-890.8961	-890.8424	0.00	33.72	-15.74	-16.60	4.1585	1.9409
0.003	-890.8969	-890.8439	0.00	33.30	-15.68	-16.21	4.1977	2.5721
0.005	-890.8982	-890.8460	0.00	32.78	-15.64	-15.87	4.3139	3.2765
0.007	-890.9000	-890.8487	0.00	32.17	-15.57	-15.60	4.5075	4.0207
0.009	-890.9023	-890.8521	0.00	31.48	-15.52	-15.39	4.7759	4.7917
0.011	-890.9051	-890.8561	0.00	30.70	-15.48	-15.25	5.1198	5.5860

Table 2. Pd-C, Pd-H, H-H bond distances (in pm) and H-H stretching wavenumber (ν_{H-H}, cm^{-1}) of the two modes of adsorption hydrogen molecule on the Pd-doped C_{20} bowl in absence and presence of external electric filed along z-axis

E_z	R(Pd-C)		R(Pd-H)		R(H-H)		ν_{H-H}	
	I	II	I	II	I	II	I	II
0.000	201.7	217.6	180.5	178.0	80.7	81.2	3480.10	3418.52
0.001	201.6	217.2	180.7	178.5	80.6	81.0	3486.27	3445.71
0.003	201.6	216.3	180.9	179.5	80.5	80.7	3496.64	3488.18
0.005	201.6	215.4	181.0	180.5	80.5	80.4	3506.32	3530.45
0.007	201.5	214.6	181.3	181.5	80.4	80.1	3519.07	3569.83
0.009	201.5	213.9	181.5	182.5	80.3	79.8	3530.59	3606.52
0.011	201.5	213.1	181.8	183.5	80.2	79.6	3544.10	3638.36

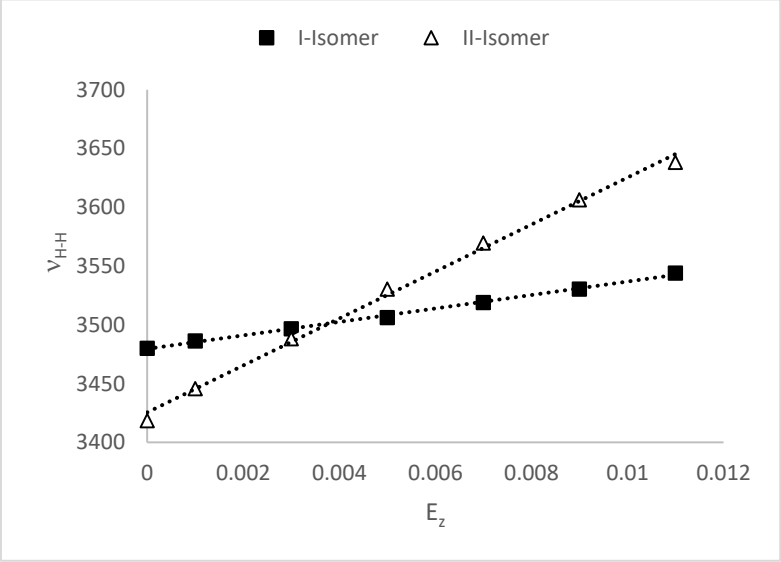

Figure 5. Linear correlations between ν_{H-H} values with EEF strength along z-axis in the various $C_{20}PdH_2$ complexes.

1. Molecular orbital analysis

Table 3 lists the HOMO-LUMO gap and the frontier orbital energy values in the evaluated systems. The values reveal that the frontier orbitals of the I-$C_{20}PdH_2$ complex are more destabilized in the EEF presence along the z-axis than in the absence. These destabilizations increase with the increasing of strength of the EEF. In the II-$C_{20}PdH_2$ complex, HOMO is destabilized in the presence EEF along the z-axis than in the absence of EEF. Such destabilization increases with an increase in the strength of the EEF along z-axis. But LUMO of the II-$C_{20}PdH_2$ complex is stabilized in the presence of EEF along the z-axis rather than in the absence of EEF. This stability increases with an elevation in the strength of the EEF along the z-axis.

The HOMO-LUMO gap value of the I-$C_{20}PdH_2$ complex increases in its presence along the z-axis than in the absence of EEF. This value increases with an increase in the strength of EEF along the z-axis. The HOMO-LUMO gap value of the II-$C_{20}PdH_2$ complex decreases in EEF presence along the z-axis than in EEF absence. Such value reduces with an increase in the strength of EEF along the z-axis.

Table 3. Frontier orbital energy and HOMO-LUMO gap values of the two modes of adsorption hydrogen molecule on the Pd-doped C_{20} bowl in absence and presence of external electric filed along z-axis (in eV).

	I		II		Gap	
E_z	E(HOMO)	E(LUMO)	E(HOMO)	E(LUMO)	I	II
0	-6.59	-3.14	-6.45	-3.37	3.45	3.09
0.001	-6.58	-3.13	-6.44	-3.38	3.45	3.07
0.003	-6.58	-3.11	-6.43	-3.40	3.47	3.03
0.005	-6.57	-3.09	-6.42	-3.43	3.49	3.00
0.007	-6.57	-3.07	-6.42	-3.45	3.50	2.96
0.009	-6.56	-3.05	-6.42	-3.49	3.52	2.93
0.011	-6.56	-3.03	-6.42	-3.52	3.53	2.89

CONCLUSION

Adsorption of hydrogen molecule on a palladium-functionalized C_{20} bowl with the B3LYP-D3 model in the absence and presence of EEF indicated that the **I**-isomer was a more stable isomer compared to the **II**-isomer. The adsorption energies exhibited that the tendency to adsorb molecules decreased with an elevation in EEF strength along the z-axis. Adsorption of hydrogen on the Pd-doped C_{20} bowl was stronger in the I-isomer than the II- isomer in the absence of EEF along the z-axis. Identical behavior was observed in the presence of EEF at 0.001-0.007 a.u. But stronger hydrogen adsorption occurred in the II-isomer than the I-isomer in the presence of EEF at 0.009-0.011 a.u. The largest wavenumber belonged to H-H stretching (ν_{H-H}). The position of this vibration was shifted to lower energy values after hydrogen adsorption occurred. Larger ν_{H-H} values were reported in the presence of EEF than in the absence of EEF. Such values increase with an increase in EEF strength along the z-axis. There are good relationships between ν_{H-H} values and EEF strength along the z-axis. The HOMO-LUMO gap value of the **I**-$C_{20}PdH_2$ complex was larger in the presence of EEF along the z-axis than in the absence of EEF. A larger gap value was found with an increase in the strength of the EEF.

REFERENCES

[1] Kannah RY, Kavitha S, Karthikeyan OP, Kumar G, Dai-Viet NV, Banu JR, Techno-economic assessment of various hydrogen production methods-A review. Bioresource Technology, 2020; 124175.

[2] Hosseini SE, Wahid MA, Hydrogen from solar energy, a clean energy carrier from a sustainable source of energy. International Journal of Energy Research, 2020; 44: 4110-4131.

[3] Barthelemy H, Weber M, Barbier F, Hydrogen storage: Recent improvements and industrial perspectives. International Journal of Hydrogen Energy, 2017; 42: 7254-7262.

[4] Lototskyy M, Tolj I, Klochko Y, Davids MW, Swanepoel D, Linkov V, Metal hydride hydrogen storage tank for fuel cell utility vehicles. International Journal of Hydrogen Energy, 2020; 45: 7958-7967.

[5] Shusheng X, Qiujie S, Baosheng G, Encong Z, Zhankuan W, Research and development of on-board hydrogen-producing fuel cell vehicles. International Journal of Hydrogen Energy, 2020; 45: 17844-17857.

[6] Afzal M, Sharma P, Design and computational analysis of a metal hydride hydrogen storage system with hexagonal honeycomb based heat transfer enhancements-part A. International Journal of Hydrogen Energy, 2021; 46: 13116-13130.

[7] Chen IN, Wu S-Y, Chen H-T, Hydrogen storage in N- and B-doped graphene decorated by small platinum clusters: A computational study. Applied Surface Science, 2018; 441: 607-612.

[8] Deniz CU, Computational screening of zeolite templated carbons for hydrogen storage. Computational Materials Science, 2022; 202: 110950.

[9] Guo C, Wang C, Remarkable hydrogen storage on Sc2B42+ cluster: A computational study. Vacuum, 2018; 149: 134-139.

[10] Papadimitriou NI, Tsimpanogiannis IN, Stubos AK, Computational approach to study hydrogen storage in clathrate hydrates. Colloids and Surfaces A: Physicochemical and Engineering Aspects, 2010; 357: 67-73.

[11] Yang J, Grzech A, Mulder FM, Dingemans TJ, The hydrogen storage capacity of mono-substituted MOF-5 derivatives: An experimental and computational approach. Microporous and Mesoporous Materials, 2013; 171: 65-71.

[12] Salehabadi A, Sarrami F, Salavati-Niasari M, Gholami T, Spagnoli D, Karton A, Dy3Al2(AlO4)3 ceramic nanogarnets: Sol-gel auto-combustion synthesis, characterization and joint experimental and computational structural analysis for electrochemical hydrogen storage performances. Journal of Alloys and Compounds, 2018; 744: 574-582.

[13] Reisi-Vanani A, Shamsali F, Influence of nitrogen doping in sumanene framework toward hydrogen storage: A computational study. Journal of Molecular Graphics and Modelling, 2017; 76: 475-487.

[14] Pichierri F, Binding of molecular hydrogen to halide anions: A computational exploration of eco-friendly materials for hydrogen storage. Chemical Physics Letters, 2012; 519-520: 83-88.

[15] Ghiasi R, Valizadeh A, Hydrogen adsorption and storage on Palladium – functionalized graphyne and its boron nitride analogue Journal of Structural Chemistry, 2021; 62: 835-844.

[16] Li X-H, Ju X-H, Density functional theory study on (Mg(BH4))n (n=1–4) clusters as a material for hydrogen storage. Computational and Theoretical Chemistry, 2013; 1025: 46-51.

[17] Chan B, Fullerene Thermochemical Stability: Accurate Heats of Formation for Small Fullerenes, the Importance of Structural Deformation on Reactivity, and the Special Stability of C60. The Journal of Physical Chemistry A, 2020; 124: 6688-6698.

[18] Fulcheri L, Schwob Y, Fabry F, Flamant G, Chibante L, Laplaze D, Fullerene production in a 3-phase AC plasma process. Carbon, 2000; 38: 797-803.

[19] Lamb LD, Huffman DR, Fullerene production. Journal of Physics and Chemistry of Solids, 1993; 54: 1635-1643.

[20] Takehara H, Fujiwara M, Arikawa M, Diener MD, Alford JM, Experimental study of industrial scale fullerene production by combustion synthesis. Carbon, 2005; 43: 311-319.

[21] Crowley C, Taylor R, Kroto HW, Walton DR, Cheng P-C, Scott LT, Pyrolytic production of fullerenes. Synthetic metals, 1996; 77: 17-22.

[22] Dubrovsky R, Bezmelnitsyn V, Eletskii A, Plasma fullerene production from powdered carbon black. Carbon, 2004; 42: 1063-1066.

[23] Montellano A, Da Ros T, Bianco A, Prato M, Fullerene C 60 as a multifunctional system for drug and gene delivery. Nanoscale, 2011; 3: 4035-4041.

[24] Shayanmehr S, Ghiasi R, Mirza B, Mohtat B, Hydrogen Adsorption and Storage on Palladium-Functionalized C_{20} Bowl and $C_{20}H_{10}$ Bowl Molecule Including Hydrogen Saturation. Journal of Structural Chemistry, 2022; 63: 1399-1408.

[25] Zahedi E, Mozaffari M, Karimi F-S, Nouri A, Density functional theory study of electric field effects on the isomerization of a photochromic molecular switch based on 1,2-dithienylethene. Can. J. Chem. , 2014; 92: 317–323

[26] Shaik S, Mandal D, Ramanan R, Oriented electric fields as future smart reagents in chemistry. Nature Chemistry, 2016; 8: 1091-1098.

[27] Shamami MK, R.Ghiasi, The analysis of OsºC bond and electric field influence on the properties in the Osmium Carbyne Complex,

$OsCl3(^{o}CCH_2CMe_3)(PH_3)_2$: A theoretical insight. J. Chinese. Chem. Soc., 2017; 64: 651–657.

[28] Ghobadi H, Ghiasi R, Jamehbozorgi S, The influence of external electric field on the electronic structure and aromaticity of Iridabenzene: a DFT study. Journal of Structural Chemistry, 2019; 60: 547-555.

[29] Zandiyeh Z, Ghiasi R, A Theoretical approach towards identification of external electric field effect on $(h^5\text{-}C_5H_5)Me_2Ta(h^2\text{-}C_6H_4)$. Russian Journal of Physical Chemistry A, 2019; 93: 482–487.

[30] Ghiasi R, Sadeghi N, Effect of external electric field on the electronic structure and aromaticity of $Cr(CO)_3(h^6\text{-}C_6H_6)$ complex Russian Journal of Inorganic Chemistry 2019; 64: 1035–1040.

[31] Kazemi Z, Ghiasi R, Jamehbozorgi S, The interaction of 5-fluorouracil with graphene in presence of external electric field: A theoretical investigation. Adsorption, 2020; 26: 905–911

[32] Liang Y, Wang F, Sun Q, Zhai Y, Molecular structural and electrical properties of trans-1,3,3,3-tetrafluoropropene and 2,3,3,3-tetrafluoropropene under external electric fields. Computational and Theoretical Chemistry, 2017; 1120: 79-83.

[33] Penfold TJ, Pápai M, Møller KB, Worth GA, Excited state dynamics initiated by an electromagnetic field within the Variational Multi-Configurational Gaussian (vMCG) method. Computational and Theoretical Chemistry, 2019; 1160: 24-30.

[34] Ghiasi R, Sofiyani MV, Emami R, Computational investigation of interaction of titanocene dichloride anti-cancer drug with carbon nanotube in presence of external electric field. Biointerface Research in Applied Chemistry, 2021; 11: 12454 - 12461.

[35] Norouzi P, Ghiasi R, Theoretical understanding the effects of external electric field on the hydrolysis of anticancer drug titanocene dichloride. Molecular Physics, 2020; 118: e1781272.

[36] Wu S, Lu L, Li L, Shi B, Tang T, Zhao X, Wei X, Tang Y, Molecular structure and excitation characteristics of DHR under different external electric fields. Computational and Theoretical Chemistry, 2022; 1215: 113810.

[37] Xia W, Zhang R, Xu X, Ma P, Ma C, Spectroscopic features and electronic properties on tetrazole-based energetic cocrystals under external electric field. Computational and Theoretical Chemistry, 2022; 1214: 113802.

[38] Xu X, Zhang R, Xia W, Ma P, Ma C, Pan Y, Jiang J, Density functional theory study of CL-20/Nitroimidazoles energetic cocrystals in an external electric field. Computational and Theoretical Chemistry, 2022; 1209: 113607.

[39] Zhou Z, Zhang X, Liu Y, Abulimiti B, Study on physical properties of ethylbenzene under external electric field. Computational and Theoretical Chemistry, 2022; 1207: 113533.

[40] Frisch MJ, Trucks GW, Schlegel HB, Scuseria GE, Robb MA, Cheeseman JR, Scalmani G, Barone V, Mennucci B, Petersson GA, Nakatsuji H, Caricato M, Li X, Hratchian HP, Izmaylov AF, Bloino J, Zheng G, Sonnenberg JL, Hada M, Ehara M, Toyota K, Fukuda R, Hasegawa J, Ishida M, Nakajima T, Honda Y, Kitao O, Nakai H, Vreven T, J. A. Montgomery J, Peralta JE, Ogliaro F, Bearpark M, Heyd JJ, Brothers E, Kudin KN, Staroverov VN, Keith T, Kobayashi R, Normand J, Raghavachari K, Rendell A, Burant JC, Iyengar SS, Tomasi J, Cossi M, Rega N, Millam JM, Klene M, Knox JE, Cross JB, Bakken V, Adamo C, Jaramillo J, Gomperts R, Stratmann RE, Yazyev O, Austin AJ, Cammi R, Pomelli C, Ochterski JW, Martin RL, Morokuma K, Zakrzewski VG, Voth GA, Salvador P, Dannenberg JJ, Dapprich S, Daniels AD, Farkas O, Foresman JB, Ortiz JV, Cioslowski J, Fox DJ *Gaussian 09*, Revision D.01; Gaussian, Inc.: Wallingford CT, 2013.

[41] Rappoport D, Furche F, Property-optimized Gaussian basis sets for molecular response calculations. The Journal of Chemical Physics, 2010; 133: 134105.

[42] Pritchard BP, Altarawy D, Didier B, Gibsom TD, Windus TL, A New Basis Set Exchange: An Open, Up-to-date Resource for the Molecular Sciences Community. J. Chem. Inf. Model., 2019; 59: 4814-4820.

[43] Feller D, The role of databases in support of computational chemistry calculations. J. Comput. Chem., 1996; 17: 1571-1586.

[44] Schuchardt KL, Karen L, Didier BT, Elsethagen T, Sun L, V. Gurumoorthi, Chase J, Li J, Windus TL, Basis Set Exchange: A Community Database for Computational Sciences. J. Chem. Inf. Model., 2007; 47: 1045-1052.

[45] Andrae D, Häußermann U, Dolg M, Stoll H, Preuß H, Energy-adjustedab initio pseudopotentials for the second and third row transition elements. Theor. Chim. Acta, 1990; 77: 123-141.

[46] Weigend F, Ahlrichs R, Balanced basis sets of split valence, triple zeta valence and quadruple zeta valence quality for H to Rn: Design and assessment of accuracy. Phys. Chem. Chem. Phys., 2005; 7: 3297.

[47] Hay PJ, Gaussian basis sets for molecular calculations. The representation of 3d orbitals in transition-metal atoms. The Journal of Chemical Physics, 1977; 66: 4377-4384.

[48] Krishnan R, Binkley JS, Seeger R, Pople JA, Self-consistent molecular orbital methods. XX. A basis set for correlated wave functions. The Journal of Chemical Physics, 1980; 72: 650-654.

[49] McLean AD, Chandler GS, Contracted Gaussian basis sets for molecular calculations. I. Second row atoms, Z=11–18. The Journal of Chemical Physics, 1980; 72: 5639-5648.

[50] Wachters AJH, Gaussian Basis Set for Molecular Wavefunctions Containing Third-Row Atoms. The Journal of Chemical Physics, 1970; 52: 1033-1036.

[51] Krishnan R, Binkley JS, Seeger R, Pople JA, Self-consistent molecular orbital methods. XX. A basis set for correlated wave functions. J. Chem. Phys., 1980; 72: 650-654.

[52] Andrae D, Häußermann U, Dolg M, Stoll H, Preuß H, Energy-adjustedab initio pseudopotentials for the second and third row transition elements. Theoretica chimica acta, 1990; 77: 123-141.

[53] Grimme S, J. Comput. Chem, 2004; 25: 1463.

[54] 54. Breneman CM, Wiberg KB, Determining atom-centered monopoles from molecular electrostatic potentials - the need for high sampling density in formamide conformational-analysis. J. Comp. Chem., 1990; 11: 361-373.

[55] S. Simon MD, Dannenberg JJ, How does basis set superposition error change the potential surfaces for hydrogen bonded dimers? J. Chem. Phys., 1996; 105: 11024-11031.